Wood Sci Technol (2017) 51:1291–1305
DOI 10.1007/s00226-017-0963-0

ORIGINAL

Effect of weight percent gain and experimental method on fiber saturation point of acetylated wood determined by differential scanning calorimetry

Leandro Passarini[1] · Samuel L. Zelinka[1] · Samuel V. Glass[1] · Christopher G. Hunt[2]

Received: 19 September 2016 / Published online: 27 September 2017

Abstract This paper evaluates the effects of acetylation level and experimental method on the observed fiber saturation point (FSP) of loblolly pine (*Pinus taeda*) wood measured using differential scanning calorimetry. To achieve this goal, 1-mm-thick latewood samples were tested over a wide range of equilibrium moisture content (EMC). In this work, the FSP was defined as the non-freezable portion of water of the samples. Two experimental methods were used: the extrapolation of the melting enthalpy to zero and the direct calculation of the non-freezable water amount. For both methods, the FSP decreased with increasing acetylation, varying from about 27% reduced EMC (EMC_R) for control to about 9% EMC_R for the highest level of acetylation. For unmodified samples, the measured FSP was higher with faster scan rates. Moreover, under a specific range of EMC_R, freezing curves revealed the occurrence of two water phase transitions for samples at the highest level of acetylation. Based on previous studies and in present findings, there is strong evidence that the lower temperature freezing peak may result from the homogenous nucleation of water, which is physically separated from water that freezes heterogeneously.

✉ Leandro Passarini
lpassari@hotmail.com

[1] Building and Fire Sciences, US Forest Service, Forest Products Laboratory, 1 Gifford Pinchot Drive, Madison, WI 53726, USA

[2] Forest Biopolymer Science and Engineering, US Forest Service, Forest Products Laboratory, 1 Gifford Pinchot Drive, Madison, WI 53726, USA

Introduction

Wood is a renewable biomaterial made up of cellulose, hemicelluloses and lignin. The water-accessible hydroxyl groups, present mainly in the hemicelluloses and amorphous portion of cellulose, are responsible for the high hygroscopicity of this material, which exchanges moisture with the surrounding environment. When subjected to large relative humidity (RH) fluctuations, the resulting swelling and shrinking of wood causes warping, checking and splitting and also compromises the performance of adhesives and surface coatings (Papadopoulos and Hill 2003; FPL 2010). To overcome these drawbacks and improve wood durability, chemical, physical or biological agents may be used to modify wood (Papadopoulos and Hill 2002; Hill 2006). During chemical modification, a reagent is covalently bound to some reactive part of wood polymers (Rowell 2013), which changes the chemical and physical properties of the material (Papadopoulos 2010).

Chemical modifications, and specifically acetylation, can reduce water sorptive properties of wood and fill spaces that water could occupy, resulting in a lower equilibrium moisture content (EMC) (Papadopoulos and Hill 2003; Papadopoulos et al. 2005; Rowell 2013; Popescu et al. 2014). Besides reducing swelling and improving dimensional stability, acetylation has been shown to increase resistance to decay (Papadopoulos and Hill 2002), termites (Papadopoulos et al. 2008a) and marine wood borers (Papadopoulos et al. 2008b). However, the exact mechanisms by which acetylation and other modifications protect wood are not fully understood and are a current topic of research (Papadopoulos and Hill 2002, 2003; Hill et al. 2005; Rowell et al. 2009; Rowell 2013; Ringman et al. 2014; Hosseinpourpia and Mai 2015; Zelinka et al. 2016a).

While the water sorption of thermally modified wood has been well characterized (Repellin and Guyonnet 2005; Almeida et al. 2009; Esteves and Pereira 2009; Olek et al. 2013; Dos Santos et al. 2014; Zanuncio et al. 2014), less information has been published on the fiber saturation point (FSP) of acetylated wood (Papadopoulos and Hill 2003; Papadopoulos et al. 2005; Hill 2008; Thygesen et al. 2010; Popescu et al. 2014; Himmel and Mai 2015). The FSP is important for understanding the influence of bound water on the physical and mechanical properties of wood. Below FSP, these properties are affected by changes in the wood moisture content (MC) (Skaar 1988; Siau 1995). There are a considerable amount of work discussing the FSP and its role on wood–water relations (Tiemann 1906; Barkas 1935; Feist and Tarkow 1967; Stone and Scallan 1967; Stamm 1971; Menon et al. 1987; Skaar 1988; Simpson and Barton 1991; Hernández and Bizoň 1994; Babiak and Kúdela 1995; Siau 1995; Berry and Roderick 2005; Almeida and Hernández 2006a, b; Hernández and Pontin 2006; Hernández 2007b; Hernández and Cáceres 2010; Telkki et al. 2013; Passarini et al. 2014, 2015; Zelinka et al. 2016b; Passarini and Hernández 2016), but only a few have drawn attention to FSP in modified wood (Hill 2008; Thybring 2013; Zauer et al. 2014). However, it has been convincingly argued that acetylated wood moisture relations should be expressed as reduced EMC (EMC_R) or reduced FSP (FSP_R), because these are calculated using only on the original wood mass, excluding the mass added during acetylation (Hill 2008; Thybring 2013).

The FSP can be theoretically defined as a transition point between water in liquid state held in wood micro-voids by capillary forces and water adsorbed in wood polymers by hydrogen bonding forces. Practically, the FSP depends upon the method used to determine it (Stamm 1971; Siau 1995; Engelund et al. 2013; Zelinka et al. 2016b). Stamm (1971) reviewed nine methods for FSP determination and reported that those involving cell wall saturation, as solute exclusion and pressure plate, gave much higher FSP values (around 40% MC), compared to those obtained from extrapolation of sorption data or changes in wood physical properties (around 25–30% MC). From this, Stamm (1971) suggested these techniques may be measuring different properties. The terms "cell wall total water capacity" (Hill 2008) for those involving saturation and "hygroscopicity limit" (Babiak and Kúdela 1995) are useful for distinguishing these methods.

Differential scanning calorimetry (DSC) is well suited to measuring FSP because it is very sensitive to the heat evolved during water phase transitions. By quantifying the enthalpy involved in phase transitions, the exact amount of water that freezes (thaws) can be calculated. The FSP can be determined by comparing the amount of water that freezes (thaws) to the total amount of water of the sample. Thus, in DSC studies, the FSP may be defined as the non-freezable portion of water of the samples (Simpson and Barton 1991; Repellin and Guyonnet 2005; Zauer et al. 2014). Several authors have used DSC to study the state of water and the FSP of various cellulosic materials (Table 1). However, a wide range of values of the FSP as determined by DSC have been reported ranging from 10.5 to 50% MC. Notably, these values span the range of both the "cell wall total water capacity" and "hygroscopicity limit."

While it is expected that pulping and thermal treatment would change FSP, it is expected that unmodified sapwoods will have similar FSP, with lower FSP for heartwood (Nearn 1955; Stamm 1964). Yet the values still range from 20 to 40% with heartwood sometimes higher in FSP than sapwood. One possible reason for these discrepancies in the FSP values found in Table 1 is that different researchers have used different experimental procedures to calculate the FSP from DSC data. In general, the procedures can be split into two major categories:

1. Extrapolation method: extrapolating the regressed values of melting enthalpy (ΔH_m) obtained as a function of EMC for FSP (or EMC_R to obtain FSP_R). In this case, the FSP corresponds to the EMC where the line intersects the ordinate, that is $\Delta H_m = 0$.
2. Direct calculation method: directly calculating the FSP from the total amount of water in the sample minus the water that undergoes a phase transition, using Eq. 1, assuming 333.6 J/g for the melting enthalpy of water (Simpson and Barton 1991).

$$\text{FSP}\ (\%) = \left(\frac{100}{m_0}\right) \times \left[\left(m_{tw} - m_{ts} \times \left(\frac{\Delta H_m}{\Delta H_{m,water}}\right)\right)\right] \quad (1)$$

here m_0 is the oven-dry mass and m_{tw} and m_{ts} are total water mass of sample (g) and

Table 1 References for DSC studies of water state and FSP on cellulosic materials

Reference	Material	FSP (%)	Method	Scan rate (°C min^{-1})
Nelson (1977)	Cellulose, pulp, paper and starch (delignified and de-bulked)	50	Extrapolation	10
Nakamura et al. (1981)	Several sources of cellulose	10.5–19.8	Direct calculation	8
Simpson and Barton (1991)	*Eucalyptus marginata* and *E. diversicolor* heartwood	32.8–33.5	Extrapolation	5 and 10
	Sapwood	34.1–37.6		
	Pinus radiata (heartwood)	32.9		
	Eucalyptus marginata and *E. diversicolor* heartwood	37.7–37.9	Direct calculation	
	Sapwood	36.7–37.9		
	Pinus radiata (heartwood)	27.8		
Repellin and Guyonnet (2005)	Untreated beech and maritime pine wood	31.7–32.9	Direct calculation	2
	Heat-treated	13.8–32.4		
Zelinka et al. (2012)	Loblolly pine solid wood (sapwood)	27	Extrapolation	5
	Cell wall components (sapwood)	20–28		
Zauer et al. (2014)	Untreated/heat-treated heartwood		Extrapolation	2
	Norway spruce	35.9/25.8		
	Sycamore maple	37.1/27.1		
	European ash	37.6/25.3		
	Untreated/heat-treated heartwood		Direct calculation	
	Norway spruce	36.3/32.1		
	Sycamore maple	37.4/30.0		
	European ash	37.1/31.5		
Mykhailyk et al. (2015)	Sprouts of poplar, willow, and alder	24.8–25.4	Extrapolation	64 (cooling)/4 (heating)

total sample mass (g), respectively. In addition to these differences in calculation methods, a wide range of scan rates and temperature ranges have been used.

In short, previous DSC studies showed a lack of consistency on the procedures to measure FSP, reflecting in a wide range of FSP values and uncertainty on the interpretation of results. Additionally, there are relatively few papers that examine the FSP of chemically modified wood. In this paper, the effect of increasing acetylation on FSP_R is examined using DSC. In addition, the effects of the DSC experimental method on FSP_R are also explored.

Materials and methods

This study was carried out using plantation grown loblolly pine (*Pinus taeda*), a species from the southern pine group. To minimize variables, all samples were latewood from the same annual ring of a commercially produced board with straight grain, free of decay and knots. Wood pieces approximately 3 mm radial × 25 mm longitudinal × 2–20 mm tangential were dried in a vacuum oven at 70 °C to a constant weight. The wood was vacuum-impregnated with acetic anhydride and then cured in an oven at 140 °C for different times. When targeting 21% weight percent gain (WPG), 4% pyridine was added to the acetic anhydride before impregnation. After reaction, samples were rinsed with water and, after sitting overnight, the remaining acetic acid and water were removed from the samples by heating in a vacuum oven for 1 h at 70 °C to determine the WPG. Less than 0.45% further weight loss from an additional 15 h of vacuum at 70 °C was observed indicating very little residual organics in the specimens. In addition, the 1-mm-thick DSC samples sat in ventilated containers for several weeks prior to testing. As expected for completely devolatilized samples, no odor was detected. The WPG of samples was calculated according to the following equation:

$$\text{WPG } (\%) = \frac{m_{\text{f}} - m_o}{m_0} \times 100 \tag{2}$$

where m_o and m_{f} are the oven-dry mass of the sample before and after acetylation, respectively.

Table 2 presents the WPGs obtained and the notation used for each condition throughout the text.

Control and modified wood were first surfaced on the longitudinal face with a sliding microtome and then cut approximately 1 mm below the surfaced side with a fine saw and jig. This was repeated until the entire specimen was consumed. These pieces were further divided with a razor blade to fit into the DSC sample pan and stored in ventilated containers for several weeks before testing began.

The samples were prepared for DSC analysis by first weighing the pan, hermetic lid and sample using an analytical balance to the nearest 0.01 mg. Considering the miniscule weight of samples (between 5 and 11 mg oven-dry) and pans (approximately 52 mg), any slight mass variation could result in a significant EMC variation. Samples were placed in the pans with the microtomed surface against the pan to maximize thermal transfer with the DSC.

Two experimental methods were compared, those used by Zelinka et al. (2012) and Zauer et al. (2014). For the twenty samples prepared following the method of

Table 2 WPG of samples and their notation

Condition	Individual specimen WPG (%)	Notation
Control	0.0	C
Acetylated	8.9	A9
	11.1, 11.6	A11
	20.8, 20.9	A21

Zelinka et al. (2012), deionized water was added to the pans using a micropipette. The amount of water was adjusted according to the desired sample EMC. The samples were then hermetically sealed and allowed to sit between 24 and 72 h prior to testing. The temperature profile began by holding the sample isothermally at 25 °C for 5 min. The temperature was then lowered at 5 °C min^{-1} until reaching − 60 °C, holding at this condition for 5 min. The temperature was then raised at 5 °C min^{-1} until reaching 25 °C again. Because a range of MCs was tested, the FSP could be calculated by both the extrapolation method and the direct calculation method. The melting enthalpy was plotted as a function of MC_R and extrapolated to $\Delta H_m = 0$ (extrapolation method). In addition, at each MC_R that exhibited a phase transition, the FSP_R was calculated from Eq. 1 (direct calculation method). For the five samples prepared following the method of Zauer et al. (2014), the samples were submerged under water for 24 h before being sealed in a sample pan and stored for 168 h prior to testing. These experiments only looked at the heating curve. The samples were cooled to − 20 °C, held for 5 min at − 20 °C and then heated to 10 °C. To examine the effect of scan rate, data were collected on these samples with scan rates of 0.5, 1, 2, 5, and 10 °C min^{-1}.

For both experiments, cooling and heating curves were obtained with a Q2000 DSC (TA Instruments, New Castle, DE) which utilized a refrigerated cooling system (RCS). The methods differed in regard to sample wetting procedure and temperature scan profiles. These procedures exactly matched the details provided in the above references. One data set, consisting of five specimens, was wetted according to one method, and the DSC scans were run according to the other method (mixed method).

After all the DSC measurements, the sample lids were perforated at multiple points and the specimens oven-dried for 24 h at 105 °C. Immediately afterward, the samples were placed inside a desiccator containing drierite™ (W.A. Hammond, Xenia, Ohio) desiccant until they cooled down. Dry masses were taken immediately upon removal from the desiccator using the same balance. The oven-dry mass obtained was used to calculate the reduced EMC (EMC_R) of samples during the DSC tests.

The EMC_R was obtained based upon the oven-dry mass before modification, excluding the mass added during acetylation (Eq. 3) (Hill 2008).

$$EMC_R(\%) = \frac{m_{ts} - m_f}{m_0} \times 100 \tag{3}$$

Thus, the FSP of acetylated wood samples was calculated, for both methods, considering EMC_R only, which is denoted FSP_R.

Data were analyzed using the Universal Analysis 2000 software, version 4.5A (TA Instruments). The heat flow (W/g) was plotted as a function of the experimental temperature (°C), and the melting enthalpy change was calculated from the area obtained below the extrapolation of the baseline before and after the water phase transition. Because of kinetic supercooling, only the melting phase transitions were used to calculate the FSP_R.

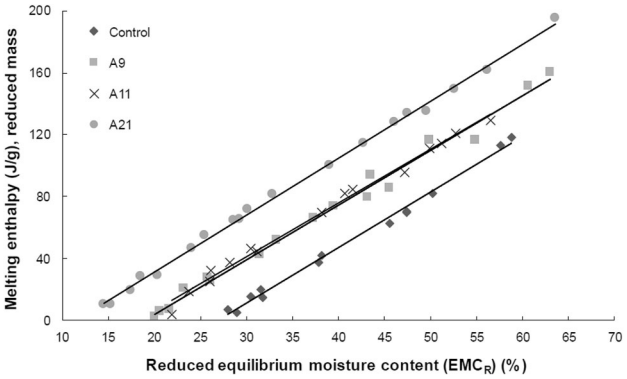

Fig. 1 Melting enthalpy as a function of the EMC_R ($n = 20$)

Table 3 Estimated FSP_R and slope obtained from the extrapolation method and direct calculation of FSP_R using the sample preparation and scan rate of Zelinka et al. (2012)

Material	Extrapolation		Direct calculation
	FSP_R (%)	Slope (J/g)	FSP_R (%)
Control	26.9 (± 0.9)[a]	357	25.9 (± 0.6)
A9	19.0 (± 1.3)	352	17.7 (± 0.8)
A11	18.3 (± 1.2)	347	17.4 (± 0.6)
A21	11.6 (± 0.7)	368	9.1 (± 0.8)

[a]Values between parentheses indicate 95% confidence interval of FSP_R

Results

Figure 1 shows the melting enthalpy (normalized to the mass of dry wood before acetylation) plotted against the EMC_R of samples. The data fit a linear relationship, with a coefficient of determination (R^2) of 99% for each of the four conditions.

Table 3 shows the average FSP_R obtained and the slope of each linear relationship. The slope represents the melting enthalpy of free water (Zelinka et al. 2012). In addition to calculating the FSP_R through the extrapolation method ($\Delta H_m = 0$), the FSP_R was also calculated by Eq. 1 for each point on the curve. This is indicated as "direct calculation" in Table 3 and assumes the melting enthalpy of free water (333.6 J g^{-1}) for all conditions.

For both calculation methods, the FSP_R decreases with increasing WPG, but the FSP_R of A9 and A11 was very similar. The extrapolation method gave higher FSP_R values than the direct calculation method, but the values were significantly different at 0.05 probability level only for A21. For all conditions, the melting enthalpy of free water (represented by the slopes) obtained in the extrapolation method was higher than the assumed 333.6 J g^{-1} in the direct calculation method.

The FSP_R values obtained by extrapolation and direct calculation for control samples were very similar and match those obtained by Zelinka et al. (2012), who

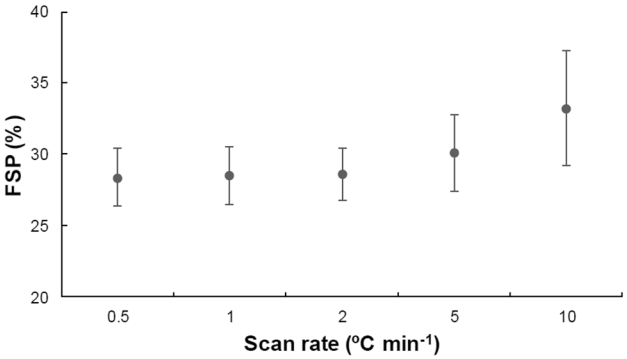

Fig. 2 FSP values obtained for control loblolly pine latewood by the sample preparation method employed by Zauer et al. (2014) at several scan rates. Error bars represent the standard error of the mean ($n = 5$)

used the extrapolation method with the same species and experimental technique. However, the FSP_R values here obtained for control samples were significantly lower than those found on untreated Norway spruce wood by Zauer et al. (2014), who used the direct calculation method, but with a different scan rate and temperature range. Zauer et al. (2014) attributed part of their higher FSP to the scan rate.

The FSP measured with the sample preparation and the direct calculation method of Zauer et al. (2014), where untreated samples were soaked for 24 h prior to treatment, are shown in Fig. 2. The FSP remained stable around 28.5% for scan rates of 0.5, 1, and 2 °C min^{-1}. However, with the increase in the scan rate to 5 and 10 °C min^{-1}, the observed FSP increased to 30.1 and 33.2%, respectively. Paired Student's *t* tests comparing data collected at 10 °C min^{-1} and 0.5, 1, or 2 °C min^{-1} all produced *p* values of 0.02 or less. However, data collected at 5 °C min^{-1} were not significantly different at 0.05 probability level (according to paired Student's *t* test) from data collected at 0.5, 1, or 2 °C min^{-1}. Importantly, all measurements, regardless of technique or scan rate, resulted in a FSP of less than or equal to 33%, near the "hygroscopicity limit," which is in contrast to the results of Zauer et al. (2014), who measured a FSP of 36.3% using the direct calculation method.

The effects of sample wetting method and scanning method on FSP are shown in Fig. 3, all based on direct calculation method and for a scan rate of 5 °C min^{-1}. Soaking the samples for 24 h in excess water reduced the apparent FSP by 1.3% relative to the pipetting method (values were not significantly different at 0.05 probability level according to paired Student's *t* test). On the other hand, scanning from − 20 to 10 °C increased the apparent FSP by 5.5% relative to scanning from − 60 to 25 °C (values were significantly different at 0.05 probability level according to paired Student's *t* test).

An unexpected feature was found on the cooling curves for A21 samples. In these curves, a second freezing peak was found in the range of 15–20% EMC_R. The melting enthalpy associated with this peak gradually decreased with the increase in EMC_R, disappearing at around 20% EMC_R. To investigate whether this was an

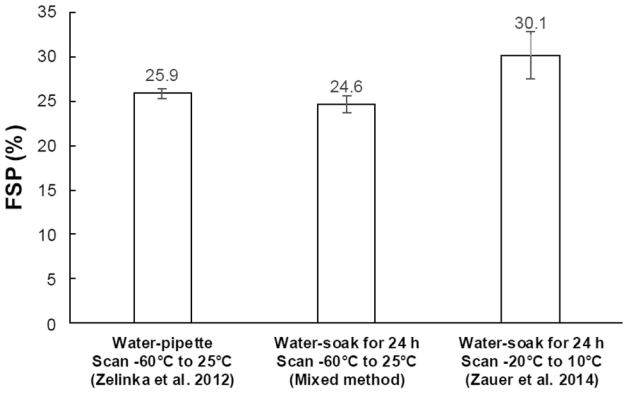

Fig. 3 Impact of experimental method on observed FSP for control loblolly pine latewood scanned at 5 °C min^{-1}, using direct calculation method. Error bars indicate 95% confidence interval of FSP ($n = 20$ for pipetted and $n = 5$ for 24 h soak)

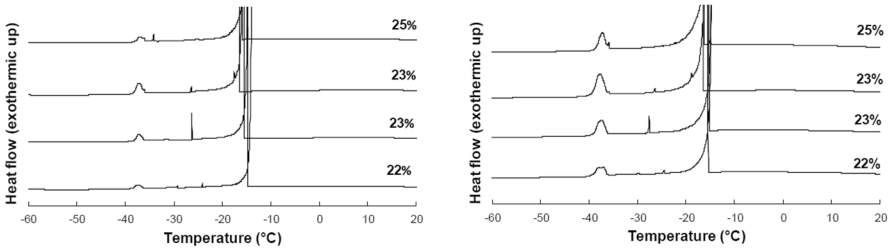

Fig. 4 Heat flow as a function of temperature obtained for A21 samples at a scan rate of 5 °C min^{-1} (left) and 10 °C min^{-1} (right), revealing two freezing peaks in the cooling curves. Each curve represents one specimen at the EMC_R listed

experimental artifact, an additional set of tests was run using five A21 samples with EMC_R varying between 22 and 27%. In this case, the method of Zelinka et al. (2012) was used, but different scan rates were tested (1, 2, 5, and 10 °C min^{-1}). Figure 4 shows representative heat flow versus temperature plots containing the two freezing peaks. The peak detected near − 40 °C (Peak II) was only detected when the scan rates were 5 or 10 °C min^{-1}. Furthermore, the freezing enthalpy associated with Peak II was slightly higher for the fastest scan rate and had no relationship to sample EMC_R.

Discussion

The FSP_R was measured with two different experimental techniques. Both techniques showed that higher WPG results in lower FSP_R. This reduction is consistent with the reduction in EMC_R of modified wood at a given RH with increasing WPG, attributed to the bulking of the cell wall by acetyl groups (Papadopoulos and Hill 2003). These acetyl groups prevent water from occupying

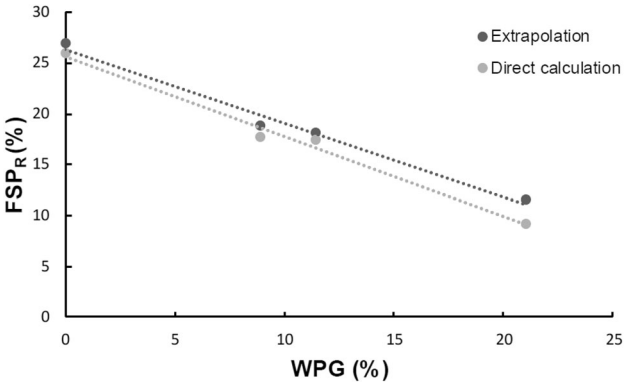

Fig. 5 Linear relationship between FSP_R and WPG ($n = 20$)

space within the cell wall by filling the available volume. NMR studies carried out by Thygesen and Elder (2008) on acetylated Norway spruce sapwood corroborated these findings. In this case, cell wall water relaxation times appeared to be lowered as result of a possible reduction in the sizes of the space available to water within cell wall due to bulking. Therefore, it was not completely unexpected that FSP_R was also lower for modified wood, especially at high WPG. Figure 5 shows a linear relationship of FSP_R with WPG, which demonstrates the relations between the decrease in the FSP_R and the degree of bulking of the cell walls. In this case, a WPG increase of 1% represents a reduction in the FSP_R of 0.73 and 0.79% calculated by extrapolation and direct calculation, respectively. Using solution exclusion to estimate FSP_R of modified Corsican pine, Hill (2008) obtained a higher FSP_R reduction, around 1% for each increase of 1% WPG.

Table 3 shows that the extrapolation method yielded higher FSP_R values than direct calculation method for all conditions, but the values were significantly different at 0.05 probability level only for A21. Both methods involve the determination of the non-freezable portion of water in the samples and consider the melting enthalpy of water. However, direct calculation considers the nominal value of melting enthalpy of free water as 333.6 J g^{-1} for all conditions, whereas those obtained experimentally by extrapolation were higher, varying between 357 for control and 368 J g^{-1} for AC21. For *Pinus radiata* heartwood, Simpson and Barton (1991) also obtained a higher FSP_R using extrapolation method (32.9%) compared to direct calculation (27.8%). Therefore, extrapolation seems to represent a higher bound for FSP_R.

As expected, the FSP_R values found in this work for the untreated samples were similar to those found by Zelinka et al. (2012), using the same species and methods. However, a recent DSC study carried out by Zauer et al. (2014) found a significantly higher FSP_R for Norway spruce heartwood, using extrapolation method (35.9%) and direct calculation (36.3%). This brought about the need to investigate the potential effects of the experimental method on FSP_R, with special attention to the effects of the scan rates. Lower scan rates may produce better resolution of the peaks, but at

the same time may also generate high levels of noise (Simpson and Barton 1991; Zauer et al. 2014).

Figure 2 shows the effects of various scan rates on measured FSP. Slow temperature scan rates produced consistent data while scans at 5 and 10 °C min^{-1} resulted in higher observed FSP. Melting enthalpy data (not shown) remained constant for scan rates of 0.5, 1, and 2 °C min^{-1} (102 J g^{-1}) and decreased to 99 and 93 J g^{-1} for 5 and 10 °C min^{-1}, respectively. It is hypothesized that as scan rates increase, there is more of a temperature gradient across the specimen, resulting in broader peaks, which are more prone to errors from imperfect baseline correction. It is believed that the fastest appropriate scan rate is highly dependent on sample thermal conduction rates and must therefore be determined for each sample geometry.

The sample wetting method had a small effect on calculated FSP, about 1.3% higher for pipetting than for soaking 24 h (Fig. 3). The temperature scanning profile, however, had a larger effect: scanning from − 20 to 10 °C increased the apparent FSP by 5.5% relative to scanning from − 60 to 25 °C (Fig. 3).

In summary, the methodology had the following effects on FSP:

- Higher scan rates yielded a higher FSP than lower scan rates.
- Scanning from − 20 to 10 °C yielded a higher FSP than scanning from − 60 to 25 °C.
- Wetting the sample by pipetting yielded a higher FSP than soaking.
- The extrapolation method yielded a higher FSP than the direct calculation method.

In short, the differences in experimental techniques cannot explain the large differences reported in the FSP between the previous works of Zauer et al. (2014) and Zelinka et al. (2012) and the current work. It is believed instead that this discrepancy might be partially explained by the different softwood species used, one naturally grown in Europe and the other in America, respectively. In the present study, only latewood was used, while Zauer et al. (2014) analyzed twin samples from the same annual rings, without mentioning if they were obtained from late or earlywood. Hernández (2007a) reported a negative relationship of wood density and EMC and thus the higher density of the latewood (FPL 2010) might also play a role in the lower FSP found in this study (FPL 2010). Considering that the lignocellulosic composition itself plays a minor role on FSP, we look to the extractive content and/or its distribution. Zauer et al. (2014) used heartwood, whereas in this study only sapwood samples were used. Heartwood is known to have a higher concentration of wood extractives (FPL 2010) and thus lower FSP_R is typically expected, the opposite of the current result. According to Hernández (2007b), extractives may have a hygroscopic, hydrophobic, or neutral behavior on wood hygroscopicity and their action may vary according to their location and distribution in the wood. Therefore, a thorough qualitative and quantitative study of the extractives in these specimens would be needed to fully understand the observed differences in FSP.

Heat flow diagrams for A21 samples sometimes exhibited a second freezing peak near − 40 °C, also called “Type II peak” (Fig. 4). This peak had been attributed to

the "freezable bound water" (Nakamura et al. 1981), or water that is partially bound to the wood cell wall but still freezes. However, Zelinka et al. (2012) did a thorough investigation of water phase transitions of loblolly pine wood and its chemical components using DSC. They found that Type II peak only appeared when samples were ball-milled prior to the study, and concluded that the high amounts of mechanical damage were affecting nucleation.

Considering that the second peak was observed only in wood that was ball-milled (Zelinka et al. 2012) or submitted to high WPG (present work), the appearance of two freezing peaks might be related to the extreme physical changes that occur to wood at high mechanical disintegration or high cell wall chemical modification. Ball-milling completely disrupts the cell wall organization and chemical bonds between cellulose (Fukazawa et al. 1982), whereas acetylation at high WPG alters the thermodynamics of the liquid water interacting with internal lumen walls (Thygesen and Elder 2008), changing contact angle and adhesion. In extreme cases, under high WPG, water droplets, rather than a film, might be formed on the lumen wall (Thygesen and Elder 2008). The second peak was observed only in samples under a short range of EMC_R above the estimated FSP_R, i.e., only 10–15% MC attributed to free water. This condition might be favorable to isolated water droplet formation. Additionally, this peak was observed only at scan rates of 5 and 10 °C min^{-1}, probably fast enough such that nucleation of water was not all heterogeneous. The actual phase transition took place at around − 40 °C, the homogeneous nucleation temperature of water. These facts reinforce the hypothesis previously advanced by Zelinka et al. (2012) that the second peak originates from homogenous nucleation of water separated physically from most of the bulk water in the specimen and is not freezable bound water.

Conclusion

The purpose of this study was to evaluate the effect of WPG and DSC experimental procedure on FSP of untreated and FSP_R of acetylated loblolly pine wood. Both FSP and FSP_R were defined as the portion of water that has no phase transitions detected in DSC heating curves. The results clearly showed that FSP_R decreased with increasing WPG. The DSC experimental methods did have a significant effect on wood FSP, especially how fast the experimental temperature changed. Scan rates lower than 5 °C min^{-1} were necessary for these samples, but appropriate scan rate should be determined for each sample type and geometry. The FSP was found to be independent of scan rate when the scan rates were between 0.5 and 2 °C min^{-1}. Additionally, how the water was added to the wood in the DSC pan affected the measured FSP. The FSP was found to be 1.3% lower when the sample had been fully submerged as opposed to having water added to it by pipetting. Scanning from − 20 to 10 °C increased the apparent FSP by 5.5% relative to scanning from − 60 to 25 °C. The extrapolation method gave slightly higher FSP and FSP_R than the direct calculation method. Other than the experimental method, high levels of WPG affected wood–water relations at some special experimental conditions. More specifically, a second peak in freezing curves was detected, attributed to the

homogenous nucleation of free water. Finally, despite the power of DSC to probe wood–water interactions, caution is needed in interpreting and extrapolating the results, since these are strongly dependent on experimental procedures and samples used are too small to be completely representative of solid wood.

References

Almeida G, Hernández RE (2006a) Changes in physical properties of tropical and temperate hardwoods below and above the fiber saturation point. Wood Sci Technol 40:599–613

Almeida G, Hernández RE (2006b) Changes in physical properties of yellow birch below and above the fiber saturation point. Wood Fiber Sci 38:74–83

Almeida G, Brito JO, Perré P (2009) Changes in wood-water relationship due to heat treatment assessed on micro-samples of three *Eucalyptus* species. Holzforschung 63:80–88

Babiak M, Kúdela J (1995) A contribution to the definition of the fiber saturation point. Wood Sci Technol 29:217–226

Barkas WW (1935) Fibre saturation point of wood. Nature 133(3414):545

Berry SL, Roderick ML (2005) Plant–water relations and the fibre saturation point. New Phytol 168:25–37

Dos Santos DVB, de Moura LF, Brito JO (2014) Effect of heat treatment on color, weight loss, specific gravity and equilibrium moisture content of two low market valued tropical woods. Wood Res Slovak 59:253–264

Engelund ET, Thygesen LG, Svensson S, Hill CAS (2013) A critical discussion of the physics of wood–water interactions. Wood Sci Technol 47:141–161

Esteves B, Pereira HM (2009) Wood modification by heat treatment: a review. BioResources 4:370–404

Feist WC, Tarkow H (1967) A new procedure for measuring fiber saturation points. Forest Prod J 17:65–68

FPL (2010) Wood handbook—wood as an engineering material. General technical report FPL-GTR-190. U.S. Department of Agriculture, Forest Service, Forest Products Laboratory, Madison, WI

Fukazawa K, Revol JF, Jurasek L, Goring DAI (1982) Relationship between ball milling and the susceptibility of wood to digestion by cellulase. Wood Sci Technol 16:279–285

Hernández RE (2007a) Moisture sorption properties of hardwoods as affected by extraneous substances, wood density, and interlocked grain. Wood Fiber Sci 39:132–145

Hernández RE (2007b) Effects of extraneous substances, wood density and interlocked grain on fiber saturation point of hardwoods. Wood Mater Sci Eng 2:45–53

Hernández RE, Bizoň M (1994) Changes in shrinkage and tangential compression strength of sugar maple below and above the fiber saturation point. Wood Fiber Sci 26:360–369

Hernández RE, Cáceres CB (2010) Magnetic resonance microimaging of liquid water distribution in sugar maple wood below fiber saturation point. Wood Fiber Sci 42:259–272

Hernández RE, Pontin M (2006) Shrinkage of three tropical hardwoods below and above the fiber saturation point. Wood Fiber Sci 38:474–483

Hill CAS (2006) Wood modification: chemical, thermal and other processes. Wiley, Chichester

Hill CAS (2008) The reduction in the fibre saturation point of wood due to chemical modification using anhydride reagents: a reappraisal. Holzforschung 62:423–428

Hill CAS, Forster SC, Farahani MRM, Hale MDC, Ormondroyd GA, Williams GR (2005) An investigation of cell wall micropore blocking as a possible mechanism for the decay resistance of anhydride modified wood. Int Biodeterior Biodegrad 55:69–76

Himmel S, Mai C (2015) Effects of acetylation and formalization on the dynamic water vapor sorption behavior of wood. Holzforschung 69:633–643

Hosseinpourpia R, Mai C (2015) Mode of action of brown rot decay resistance of acetylated wood: resistance to Fenton's reagent. Wood Sci Technol 50:413–426

Menon RS, MacKay AL, Hailey JRT, Bloom M, Burgess AE, Swanson JS (1987) An NMR determination of the physiological water distribution in wood during drying. J Appl Polym Sci 33:1141–1155

Mykhailyk VA, Snezhkin YF, Dmitrenko NV (2015) Investigation of the state of water in energy trees in the process of drying by differential scanning calorimetry. J Eng Thermophys 88:1093–1099
Nakamura K, Hatakeyama T, Hatakeyama H (1981) Studies on bound water of cellulose by differential scanning calorimetry. Text Res J 51:607–613
Nearn WT (1955) Effect of water soluble extractives on the volumetric shrinkage and equilibrium moisture content of eleven tropical and domestic woods. Pennsylvania State University, College of Agriculture, Bulletin 598, State College
Nelson RA (1977) The determination of moisture transitions in cellulosic materials using differential scanning calorimetry. J Appl Polym Sci 21:645–654
Olek W, Majka J, Czajkowski Ł (2013) Sorption isotherms of thermally modified wood. Holzforschung 67:183–191
Papadopoulos AN (2010) Chemical modification of solid wood and wood raw material for composites production with linear chain carboxylic acid anhydrides: a brief review. BioResources 5:499–506
Papadopoulos AN, Hill CAS (2002) The biological effectiveness of wood modified with linear chain carboxylic acid anhydrides against *Coniophora puteana*. Holz Roh Werkst 60:329–332
Papadopoulos AN, Hill CAS (2003) The sorption of water vapour by anhydride modified softwood. Wood Sci Technol 37:221–231
Papadopoulos AN, Avramidis S, Elustondo D (2005) The sorption of water vapour by chemically modified softwood: analysis using various sorption models. Wood Sci Technol 39:99–112
Papadopoulos AN, Avtzis D, Avtzis N (2008a) The biological effectiveness of wood modified with linear chain carboxylic acid anhydrides against the subterranean termites *Reticulitermes flavipes*. Holz Roh Werkst 66:249–252
Papadopoulos AN, Duquesnoy P, Cragg SM, Pitman AJ (2008b) The resistance of wood modified with linear chain carboxylic acid anhydrides to attack by the marine wood borer *Limnoria quadripunctata* Hothius. Int Biodeterior Biodegrad 61:199–202
Passarini L, Hernández RE (2016) Effect of the desorption rate on the dimensional changes of *Eucalyptus saligna* wood. Wood Sci Technol 50:941–951
Passarini L, Malveau C, Hernández RE (2014) Water state study of wood structure of four hardwoods below fiber saturation point with NMR technique. Wood Fiber Sci 46:480–488
Passarini L, Malveau C, Hernández RE (2015) Distribution of the equilibrium moisture content in four hardwoods below fiber saturation point with magnetic resonance microimaging. Wood Sci Technol 49:1251–1268
Popescu CM, Hill CAS, Curling S, Ormondroyd G, Xie Y (2014) The water vapour sorption behaviour of acetylated birch wood: how acetylation affects the sorption isotherm and accessible hydroxyl content. J Mater Sci 49:2362–2371
Repellin V, Guyonnet R (2005) Evaluation of heat-treated wood swelling by differential scanning calorimetry in relation to chemical composition. Holzforschung 59:28–34
Ringman R, Pilgård A, Brischke C, Richter K (2014) Mode of action of brown rot decay resistance in modified wood: a review. Holzforschung 68:239–246
Rowell RM (2013) Handbook of wood chemistry and wood composites, 2nd edn. CRC Press, Boca Raton
Rowell RM, Ibach RE, McSweeny J, Nilsson T (2009) Understanding decay resistance, dimensional stability and strength changes in heat-treated and acetylated wood. Wood Mater Sci Eng 4:14–22
Siau JF (1995) Wood: Influence of moisture on physical properties. Virginia Polytechnic Institute and State University, Virginia
Simpson L, Barton AFM (1991) Determination of the fibre saturation point in whole wood using differential scanning calorimetry. Wood Sci Technol 25:301–308
Skaar C (1988) Wood-water relations. Springer, Berlin
Stamm AJ (1964) Wood and cellulose science. The Ronald Press Co, New York
Stamm AJ (1971) Review of nine methods for determining the fiber saturation point of wood and wood products. Wood Sci 4:114–128
Stone JE, Scallan AM (1967) The effect of component removal upon the porous structure of the cell wall of wood II. Swelling in water and the fiber saturation point. Tappi 50:496–501
Telkki VV, Yliniemi M, Jokisaari J (2013) Moisture in softwoods: fiber saturation point, hydroxyl site content, and the amount of micropores as determined from NMR relaxation time distributions. Holzforschung 67:291–300
Thybring EE (2013) The decay resistance of modified wood influenced by moisture exclusion and swelling reduction. Int Biodeterior Biodegrad 82:87–95

Thygesen LG, Elder T (2008) Moisture in untreated, acetylated, and furfurylated Norway spruce studied during drying using time domain NMR. Wood Fiber Sci 40:309–320

Thygesen LG, Engelund ET, Hoffmeyer P (2010) Water sorption in wood and modified wood at high values of relative humidity. Part I: results for untreated, acetylated, and furfurylated Norway spruce. Holzforschung 64:315–323

Tiemann HD (1906) Effect of moisture upon the strength and stiffness of wood. USDA Forest Service, Bulletin 70, Washington

Zanuncio AJV, Motta JP, da Silveira TA, Farias ES, Trugilho PF (2014) Physical and colorimetric changes in *Eucalyptus grandis* wood after heat treatment. BioResources 9:293–302

Zauer M, Kretzschmar J, Großmann L, Pfriem A, Wagenführ A (2014) Analysis of the pore-size distribution and fiber saturation point of native and thermally modified wood using differential scanning calorimetry. Wood Sci Technol 48:177–193

Zelinka SL, Lambrecht MJ, Glass SV, Wiedenhoeft AC, Yelle DJ (2012) Examination of water phase transition in Loblolly pine and cell wall components by differential scanning calorimetry. Thermochim Acta 533:38–45

Zelinka SL, Ringman R, Pilgård A, Thybring EE, Jakes JE, Richter K (2016a) The role of chemical transport in the decay resistance of modified wood. Int Wood Prod J 7:66–70

Zelinka SL, Glass SV, Jakes JE, Stone DS (2016b) A solution thermodynamics definition of the fiber saturation point and the derivation of a wood–water phase (state) diagram. Wood Sci Technol 50:443–462